Applied Catalysis B: Environmental 198 (2016) 189–199

Contents lists available at ScienceDirect

Applied Catalysis B: Environmental

journal homepage: www.elsevier.com/locate/apcatb

NOx storage and reduction over copper-based catalysts. Part 1: BaO + CeO_2 supports

Agustín Bueno-López [a,b,*,1], Dolores Lozano-Castelló [a,b], James A. Anderson [b]

[a] MCMA Group, Inorganic Chemistry Department, University of Alicante, Spain
[b] Surface Chemistry and Catalysis, Materials and Chemical Engineering Group, School of Engineering, University of Aberdeen, UK

ARTICLE INFO

Article history:
Received 11 April 2016
Received in revised form 24 May 2016
Accepted 27 May 2016
Available online 27 May 2016

Keywords:
NSR
deNOx
Diesel aftertreatment
Copper catalyst
Ceria
Barium oxide
DRIFTS
Operando

ABSTRACT

The performance of noble metal-free copper-based NSR catalysts was studied by rapid-scan *operando* DRIFTS, using CeO_2, BaO and BaO + CeO_2 mixtures with different ratios as supports. The maximum temperature for CuO/CeO_2 utilization as NSR catalyst was 400 °C, as the stored NOx species decomposed above this temperature. At 400 °C, CuO/CeO_2 showed high NO oxidation capacity and NOx were stored on the catalyst mainly in the form of nitrates and lower populations of nitro groups. CuO/BaO was not suitable for NSR below 250 °C, because its oxidation activity was very low and its NOx storage capacity was negligible, but it did not exhibit upper temperature restrictions until 500 °C. The effect of temperature on NOx chemisorption on copper catalysts with BaO + CeO_2 mixed oxide supports was between those of CuO/CeO_2 and CuO/BaO. NSR experiments performed with high frequency H_2 or CO pulses (micropulses every 120, 60 or 30 s) at 400 °C showed that regeneration with H_2 was more effective than with CO, and this was attributed to the higher reactivity of H_2 rather than to the poisoning effect of the reaction products (H_2O and CO_2 respectively). Nitrates were the main form of chemisorbed nitrogen oxides on all catalysts in NSR experiments at 400 °C, and NOx chemisorption and desorption rates were faster for CuO/CeO_2 than for CuO/BaO. The general behavior of all catalysts tested for NSR at 400 °C was quite similar, and only certain differences were observed during the highest frequency pulses of CO, where CuO/CeO_2 showed the best resistance to deactivation. For all catalysts, N_2 was the only NOx reduction product detected during H_2 regeneration.

1. Introduction

Diesel engine exhausts are net oxidizing, and NOx reducing under such unfavorable conditions is a current challenge of ongoing research. The NOx Storage and Reduction (NSR) strategy is one of the options for NOx removal from diesel exhausts, which operates under cyclic oxidizing and reducing conditions [1–4]. A typical NSR catalyst includes a basic oxide that chemisorbs NOx under normal running conditions, and periodically, a reductant is fed to the exhaust that desorbs and reduces the stored NOx. Barium oxide is the most studied basic oxide for NSR catalysts. Pt is also included in the catalyst formulation to accelerate NO oxidation to NO_2, hence improving NOx chemisorption, and to catalyze further reduction [4]. The most convenient reductants for NSR would be hydrocarbons, because fuel is already on board. However, their reactivity is usually not high [5] and CO + H_2 mixtures are more suitable [6], and these can be produced on board by steam reforming, water gas shift reaction, partial oxidation, or autothermal reforming [4].

It has been recently reported that the NSR behavior of Ba-Pt/Al_2O_3 catalyst is improved by addition of ceria, because ceria enhances the NOx storage capacity and the NO oxidation activity [7]. It has been also observed that addition of ceria to Pt-Ba/Al_2O_3 catalysts has a positive effect on NOx reduction with H_2, because it lowers the thermal threshold for hydrogen activation. The utilization of CeO_2 [8,9] or CeZr mixed oxides [9,10] instead of Al_2O_3 as Pt + BaO supports has been also studied for NSR application, and also barium-free Pt/$Ce_xPr_{1-x}O_2$ catalysts [11].

The potential of noble metal-free NSR catalysts has not been studied in detail in the literature, and this is one of the goals of the current study. This would have practical relevance to lower the price of the catalysts and to decrease the dependence of noble metals. Vijay et al. [12] found that a noble metal-free Co-Ba catalyst was able to store NOx as efficiently as a Pt-Ba NSR catalyst, and Palomares et al. [13] reported that Mg/Al hydrotalcites containing copper or cobalt are active for low temperature NSR, and that an optimum formulation with Co/Mg/Al = 15/60/25 outperformed a reference Pt–Ba/Al_2O_3 catalyst. The promoting effect of CuZSM-5 to the NSR activity of Pt–Rh/Ba/Al_2O_3 was also demonstrated [14],

* Corresponding author at: Carretera de San Vicente s/n. E03080, Alicante, Spain.
E-mail address: agus@ua.es (A. Bueno-López).
[1] http://personal ua es/es/agu.

http://dx.doi.org/10.1016/j.apcatb.2016.05.067
0926-3373/

and the promising behavior of copper-containing $SrTiO_3$ perovskite as NSR catalyst has been reported [15]. In these NSR catalysts, copper improves the NO oxidation capacity and NOx are stored on the mixed oxide.

This article is the first in a series devoted to the study of noble metals-free copper catalyst for NSR. In this article, the effect of CeO_2, BaO and BaO + CeO_2 supports on the NSR behavior of copper has been studied by *operando* DRIFTS-MS-Chemiluminiscence, paying special attention to the reaction mechanism. Realistic periods of lean operation (30–120 s) similar to those originally proposed by Toyota in the mid 90 s [16] and periodic micropulses of reductant were used. This detail is significant when making comparison with other studies because, as has been highlighted by other authors [17], despite the high level of activity in this area, it is surprising that most studies have been conducted with much longer lean periods and regeneration times, which are far from realistic conditions. Rapid-scan operando DRIFTS experiments were performed in a spectrometer that is able to obtain up to 17 spectra per second. This novel methodology has recently demonstrated to be very powerful to study the NSR reaction when performed with high frequency micropulses [18].

Further articles in this series will be devoted to the study of the effect of Zr, La, Pr and Nd dopants on the NSR performance of CuO/CeO_2 NSR catalysts, and on the simultaneous removal of NOx and soot with Pr-doped CuO/CeO_2 under NSR conditions.

2. Experimental details

2.1. Catalysts preparation

xBaO + (1-x)CeO_2 supports were prepared with x = 1, 0.8, 0.6, 0.4, 0.2 and 0 with $Ce(NO_3)_3{\cdot}6H_2O$ (Alfa-Aesar, 99.5%) and $Ba(OH)_2{\cdot}8H_2O$ (Panreac) as Ce and Ba precursors, respectively. Aqueous dissolutions of the Ce and Ba precursors were prepared with 10 ml of solvent, using the required amounts to obtain 5 g of each mixed oxide. The dissolutions were introduced in a muffle furnace previously heated at 200 °C, and after 1 h, the temperature was increased at 10 °C/min until 500 °C, holding the samples at this temperature for 2 h. The nomenclature used for the xBaO + (1-x)CeO_2 supports is "xBaO-(1-x)CeO_2" where x and (1-x) are the percentages of BaO and CeO_2, respectively.

CuO/(xBaO-(1-x)CeO_2) catalysts were prepared with a 5 wt.% target Cu loading. The required amount of $Cu(NO_3)_2{\cdot}5{\cdot}(1/2)H_2O$ (Sigma Aldrich, 98%) was dissolved in 2 ml of water and 2.5 g of each (xBaO-(1-x)CeO_2) support was impregnated with this solution. The impregnated supports were heat treated following the same protocol used for the supports preparation, that is, they were introduced in a muffle furnace previously heated at 200 °C, and after 1 h, the temperature was increased at 10 °C/min until 500 °C, holding this temperature for 2 h.

2.2. Catalyst characterization

The catalysts were characterized by XRD and by N_2 adsorption at −196 °C. X-Ray diffractograms were recorded from 10 to 90° 2θ in a Bruker D8 advance diffractometer using CuKα radiation (λ = 0.15418 nm). N_2 adsorption isotherms were obtained at −196 °C in an automatic volumetric system (Autosorb-6, Quantachrome) after the catalysts were degassed at 150 °C for 4 h.

2.3. NOx chemisorption and NSR experiments

NOx chemisorption and NSR performance were studied in a Fourier Transform Infrared Spectrometer Shimadzu (IR Tracer-100) with a Harrick reaction cell coupled to a EcoSys-P mass spectrometer and a chemiluminiscence NOx analyzer (Thermo 42H). The sample holder of the DRIFT cell was 6.3 mm diameter with a height of 3.3 mm which was filled with sample (100 mg in the absence of diluent). It is important to note that the infrared spectrum only provides information on the top < 0.2 mm of this sample [19].

The reaction cell was designed to allow the reaction gas mixture (50 ml/min; 850 ppm NOx + 5% O_2 + N_2) to pass through the catalyst bed with the gas exit underneath.

It is worth mentioning that temperature control and determination in DRIFTS cells is problematic. It has been reported that the actual temperature of the catalyst bed can be significantly lower than the set temperature, with differences of around 50 °C when operating at 400 °C [20]. This must be kept in mind when cross referring to data obtained using other devices including reactors.

Three types of experiments were carried out: Temperature programmed NOx storage experiments, isothermal NOx storage at 400 °C and Isothermal NOx Storage and Reduction (NSR) at 400 °C.

In temperature programmed NOx storage experiments, a background spectrum of the catalyst was recorded at room temperature, and the $NOx/O_2/N_2$ mixture was fed to the DRIFTS cell. After 15 min, the temperature was increased at 10 °C/min until 500 °C and DRIFT spectra and chemiluminescence NOx measurements were simultaneously recorded. 40 scans were averaged to obtain each spectrum, which were measured in the 4000–1000 cm^{-1} range at 4 cm^{-1} resolution.

In isothermal NOx storage experiments at 400 °C, the temperature was increased from room temperature to 400 °C under N_2. A background spectrum of the catalyst was recorded at 400 °C, and then the inert gas was replaced by the $NOx/O_2/N_2$ mixture, considering this as time = 0 min. DRIFT spectra and chemiluminescence NOx measurements were simultaneously recorded with time until saturation of the catalysts. In these experiments, the settings used to obtain the spectra were the same as in previous temperature programmed NOx storage experiments.

Isothermal NOx storage and reduction (NSR) experiments were carried out following the protocol described for isothermal NOx storage experiments at 400 °C, but in addition, 100 μl pulses of CO or H_2 were fed with frequencies of 120, 60 or 30 s. These times are in the range of realistic values for application of the NSR technology, as developed by Toyota [16,17,21]. In these experiments, the DRIFT spectrometer was operated in the rapid-scan mode, and one spectrum was recorded per second as an average of 7 scans, which were recorded with a resolution of 8 cm^{-1} in the 4000–1000 cm^{-1} range. The Rapid-scan Software (Shimadzu Corporation) was used to handle the large volume of data generated. The gas composition was monitored during these experiments with the mass spectrometer. This technique was used in preference to chemiluminiscence because the sampling frequency of the mass spectrometer was much faster. Previous comparison of the NOx concentrations measured by chemiluminiscence and mass spectrometry (m/z 30) confirmed that both techniques provided comparable results. The benefit of chemiluminiscence is that it is able to distinguish between NO and NO_2 while the m/z 30 signal shows the NOx sum (i.e. NO + NO_2).

3. Results and discussion

3.1. Catalysts characterization

X-Ray diffractograms of the catalysts were compiled in Fig. 1, along with the cell parameter of the fluorite phase of ceria, calculated from these diffractograms, together with the BET surface areas calculated from the N_2 adsorption isotherms (Table 1). The diffractogram of the CuO/CeO_2 catalyst showed the peaks of fluorite, which is the cubic phase of ceria, and evidence of CuO peaks were not observed on this catalyst indicating high dispersion. On

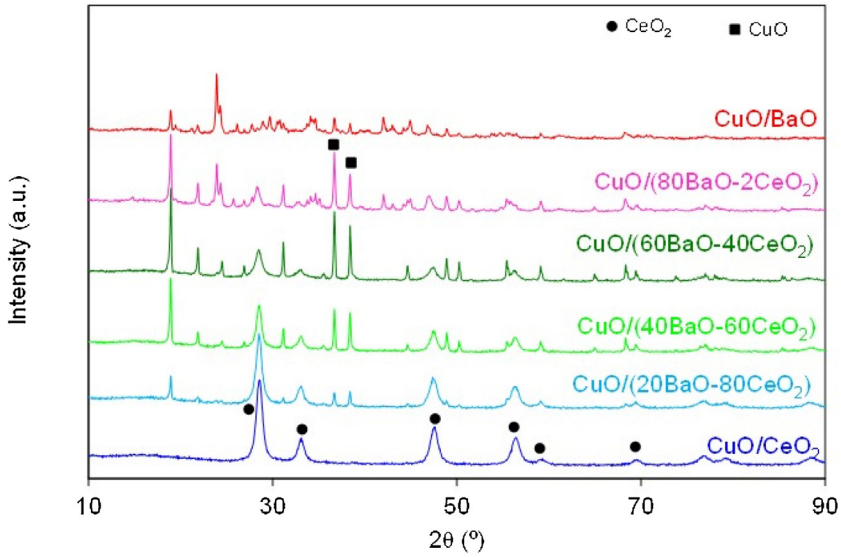

Fig. 1. X-Ray difractograms of the catalysts.

Table 1
BET surface area of the catalysts and fluorite cell parameter.

Catalyst	BET (m^2/g)	Fluorite cell parameter(nm)
CuO/CeO_2	60	0.5411
$CuO/(20BaO\text{-}80CeO_2)$	30	0.5414
$CuO/(40BaO\text{-}60CeO_2)$	11	0.5420
$CuO/(60BaO\text{-}40CeO_2)$	13	0.5420
$CuO/(80BaO\text{-}20CeO_2)$	1	0.5429
CuO/BaO	1	–

the contrary, CuO peaks were identified in all barium-containing catalysts, and this indicated that copper was more poorly dispersed. This is consistent with the decrease of the BET surface area of the catalysts (Table 1) by increasing the BaO loading, which decreases from 60 m^2/g for the CuO/CeO_2 catalyst to 1 m^2/g for CuO/BaO. The difractogram of CuO/BaO is complex and included peaks of several barium species such as BaO, $BaCO_3$ and $Ba(OH)_2$, and the catalysts with $(xBaO\text{-}(1\text{-}x)CeO_2)$ supports show features of both CuO/BaO and CuO/CeO_2. The cell parameter values of the fluorite phase of ceria included in Table 1 were quite similar for all samples, and were consistent with typical reference values obtained with pure ceria [22], suggesting limited or no insertion of barium cations into the ceria framework.

In conclusion, these characterization suggested that the $(xBaO\text{-}(1\text{-}x)CeO_2)$ supports consisted of a mixture of oxides, carbonates and hydroxides that did not form solid solutions. The surface area of CeO_2 was much higher than that of BaO, and $(xBaO\text{-}(1\text{-}x)CeO_2)$ mixed oxides had surface areas that decreased with the BaO content. This affected CuO dispersion, which was much better on CeO_2 than on barium-containing supports.

3.2. Temperature programmed NOx storage experiments

Temperature programmed experiments were performed and the copper catalysts studied, once in contact with the $NOx/O_2/N_2$ gas flow, chemisorbed NOx and accelerated the oxidation of NO to NO_2. Fig. 2 shows (a) the NOx concentration and (b) the percentage of NO_2 with regard to total $NO + NO_2$ monitored with the chemiluminiscence NOx analyzer during the temperature programmed NOx storage experiments.

Different ranges of temperatures could be distinguished considering the NOx profiles (Fig. 2a). NOx concentrations below the inlet level were detected for $CuO/(xBaO\text{-}(1\text{-}x)CeO_2)$ catalysts

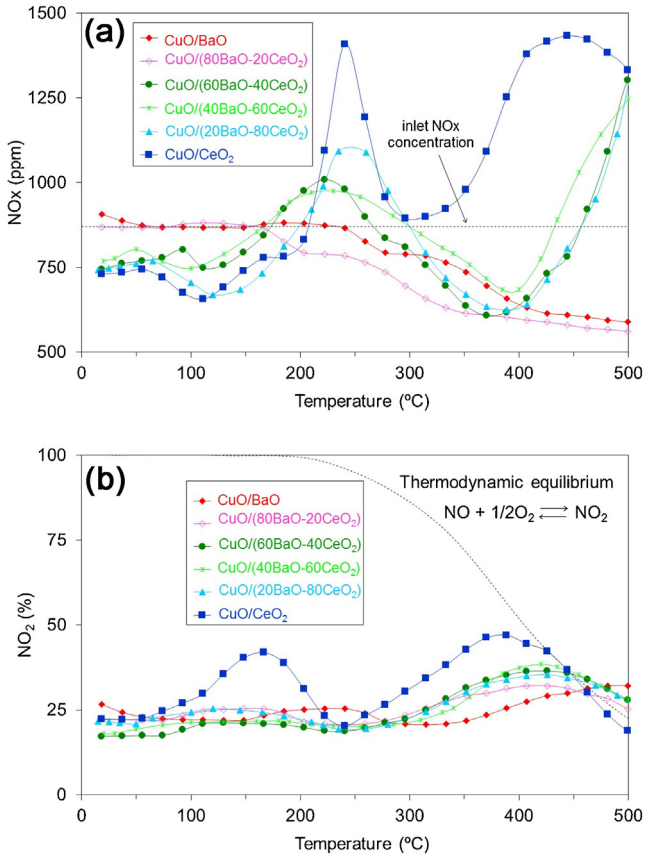

Fig. 2. NOx concentration (a) and NO_2 percentage with regard to total $NO + NO_2$ (b) monitored with the chemiluminiscence NOx analyzer during the Temperature Programmed NOx Storage experiments. (Gas mixture with 850 ppm $NOx + 5\%O_2 + N_2$).

with $x \leq 60\%$ at temperatures below 200 °C. That is, these catalysts removed NOx from the gas mixture in this range of temperatures. Note that the catalysts were in contact with the $NOx/O_2/N_2$ mixture for 15 min at room temperature, and NOx was also adsorbed on the catalysts during this period of time. On the contrary, the barium-rich CuO/BaO and $CuO/(80BaO\text{-}20CeO_2)$ catalysts did not store NOx at low temperature, and therefore, it was concluded that

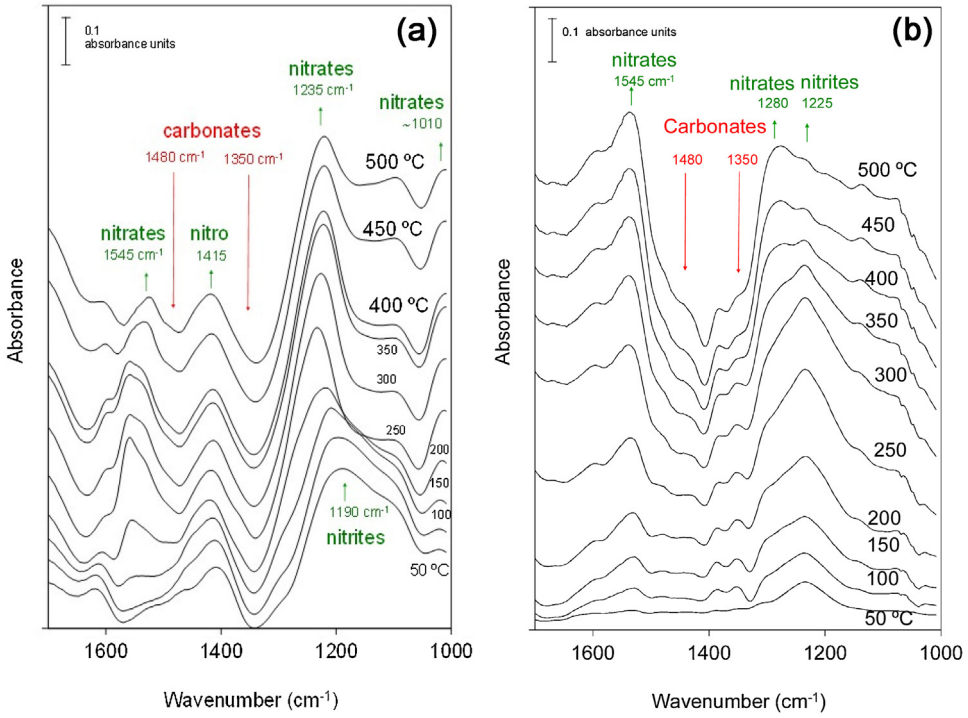

Fig. 3. Spectra obtained with CuO/CeO_2 (a) and CuO/BaO (b) and recorded during the Temperature Programmed NOx Storage experiments. (Gas mixture with 850 ppm NOx + 5%O_2 + N_2).

the presence of cerium was necessary for the catalysts to store NOx below 200 °C. This could be related to the very low surface area of these two catalysts (1 m^2/g; Table 1), which was too low to adsorb significant amounts of NOx.

The catalysts that stored NOx below 200 °C (CuO/(xBaO-(1-x)CeO_2 with $x \leq 60\%$) released NOx in the range 200–300 °C, indicating low thermal stability of the species adsorbed at low temperature, and CuO/CeO_2 additionally released NOx above 300 °C. All barium-containing catalysts chemisorbed NOx above 300 °C but, while catalysts with cerium contents in the $20\% \leq x \leq 60\%$ range released NOx above 450 °C, CuO/BaO and CuO/(80BaO-20CeO_2) continued to chemisorb until the maximum temperature of the experiments (500 °C).

The catalytic oxidation of NO to NO_2 took place simultaneously during NOx chemisorption/desorption (Fig. 2). NO_2 is the most thermodynamically stable nitrogen oxide at room temperature, but the oxidation of NO is kinetically restricted and requires long times for NO to become oxidized to NO_2 in the absence of catalyst. NO_2 was present at 20–25% at room temperature for all experiments, and it was experimentally confirmed that this was the amount of NO converted to NO_2 in the experimental set-up without catalyst participation.

CuO/CeO_2 was the most active catalyst for NO oxidation to NO_2, with an onset NO_2 release temperature of 100 °C under the experimental conditions employed. This is consistent with the conclusions of Pereda-Ayo et al. [7], who reported that ceria improved the NO oxidation capacity of model Ba-Pt/Al_2O_3 catalysts, and this enhanced the NOx storage capacity of the catalysts. The NO_2 curve obtained with CuO/CeO_2 (Fig. 2b) decreased above 175 °C, and this is not attributed to the decrease of the NO oxidation capacity of CuO/CeO_2 (reaction rate increases with temperature) but to the desorption of NOx stored at lower temperature (compare Figs. 2a and b). Considering typical experimental conditions used in fixed-bed reactors [23] it would be expected that the NO_2 percentage should increase with temperature until the thermodynamic limitation is achieved, and above this temperature, the NO_2 profile should follow the thermodynamically predicted curve. The high temperature part of the expected curve was observed in Fig. 2b, and the NO_2 percentage followed the values defined by thermodynamic equilibrium above 400 °C, but part of the NO_2 curve was absent between 170 and 450 °C. The difference in the NO_2 profile observed in the DRIFTS cell and in previous experiments performed in a fixed-bed reactor [23] was the space velocities employed, being much lower in the DRIFTS cell. For this reason, the effect of NOx desorption in the NO_2 profiles was minor or negligible for experiments performed under the experimental conditions typically used in fixed-bed reactors, but not for those used in the DRIFTS cell.

With the exception of CuO/CeO_2, the remaining catalysts showed very low NO oxidation capacity (Fig. 2b), with onset NO_2 release temperatures above 300 °C, and this could be related to the poor copper dispersion. For most catalysts, NOx chemisorption and NO_2 formation were coupled, that is, NOx chemisorption started at 300 °C (Fig. 2a), once NO_2 was detected in the gas phase due to catalytic oxidation of NO (Fig. 2b). This was not surprising because NO_2 is usually chemisorbed more readily than NO [24], and NSR catalysts typically chemisorb NOx to a greater extent once the temperature is high enough for catalytic oxidation of NO to take place.

As a summary of NO oxidation and storage results (Figs. 2a and b), it can be concluded that CuO/CeO_2 was much more effective than CuO/BaO for NOx storage and NO oxidation at low temperature, but the stored species were less stable, being desorbed above 200 °C. On the contrary, CuO/BaO required higher temperatures for NOx chemisorption than CuO/CeO_2 but the stored species remained stable until 500 °C (at least). The behavior of CuO/(xBaO-(1-x)CeO_2) catalysts was in between, with catalysts of high barium concentration behaving more similarly to CuO/BaO while those with high cerium concentration showed more commonality with CuO/CeO_2.

The adsorbed NOx species on the catalysts were monitored by DRIFTS during temperature programmed NOx storage experiments. As representative examples of the spectra obtained, data for CuO/CeO_2 and CuO/BaO are shown in Fig. 3a and b, respectively and

the spectra of the remaining catalysts are included in the supplementary material (Fig. 1SM). In all sets of spectra, bands attributed to nitrogen-containing species grew with increasing temperature while carbonate bands decreased as nitrogen oxides replaced carbonates. This general observation can be extended to all catalysts with ($xBaO$-$(1-x)CeO_2$) supports (not shown for sake of brevity). The possibility of cleaning the catalysts surface before conducting experiments by removing carbonates with a thermal treatment was explored. Carbonate removal was possible for CuO/CeO_2, but not for barium-rich catalysts due to the very high temperatures required which might also have modified catalysts characteristics and may have been beyond the limit of the temperature maxima of the DRIFTS cell. For this reason, the presence of carbonates on all catalysts which would be formed upon exposure to atmospheric CO_2 was assumed. This has some practical significance as carbonates will always be present under real NSR operation conditions, and there has been debate regarding the role of carbonates on the performance of $Pt/BaO/Al_2O_3$ model NSR catalysts [25] that justifies the study of carbonated samples.

Before discussing the behavior of the different bands of nitrogen species observed in Fig. 3 in detail, it is worth mentioning that it has been recently reported that the molar absorption coefficients of the overlapping bands due to carbonates and nitrates are not identical. For this reason, the true position of the nitrate and nitrite bands cannot be assessed form such complex spectra [26,27]. However, despite this limitation, some general conclusions can be reached while bearing in mind that the position of the nitrite and nitrate bands in the following discussion may differ to some extent from those described for other carbonate-free systems.

Nitrates show three bands in the 1650–970 cm^{-1} range, and the position of these bands depends on the surface to which they are anchored and on the bonding arrangement with the surface (monodentate (M-O-NO_2), bidentate (M-O_2NO) or bridging ((M-$O)_2$ = NO), M being a metal cation) [28]. In the spectra obtained with the CuO/CeO_2 catalyst (Fig. 3a), nitrate bands appeared at 1545, 1235 and 1010 cm^{-1}, and are consistent with the presence of monodentate or bidentate nitrates. This catalyst also showed a band at 1415 cm^{-1} that could be assigned to nitro groups (M-NO_2) and, at low temperatures, a band at 1190 cm^{-1} that could be attributed to bridging nitrites ((M-$O)_2$ = N). In addition, evidence of carbonate depletion was observed in this wavenumber range. The antisymmetric and symmetric stretching modes of the terminal CO bonds in poly or mono-dentate carbonates usually appear around 1480 and 1350 cm^{-1}, respectively [29], and these features were observed in the spectra of CuO/CeO_2.

The CuO/BaO catalyst (Fig. 3b) did not show evidence of nitro groups, but instead, features at 1535 and 1280 cm^{-1} could be attributed to nitrates, probably in monodentate configuration, and as bridging nitrites at 1225 cm^{-1} at low temperatures. In this case, the depletion of carbonates also had a strong influence on the spectra in the 1500–1300 cm^{-1} range.

Quantitative analysis of the spectra was hindered due to the depletion of carbonate species which led to diminishing band intensities while those of the nitrogen oxide groups were simultaneously increased. The intensity of the band due to nitrites appearing around 1225–1190 cm^{-1} can be properly estimated without significant influence by carbonates, and the values obtained were plotted as a function of temperature (Fig. 4a) after baseline correction. The absorbance at 1280–1235 cm^{-1} was selected for monitoring nitrates (Fig. 4b), but in this case the possibility that data are partially masked by carbonate depletion in some spectra cannot be ruled out. These data where evidence of interference due to carbonates is apparent are plotted in Fig. 4 with dashed lines and open symbols.

Nitrites were progressively accumulated on CuO/CeO_2 from room temperature until *ca* 150 °C, and above this temperature

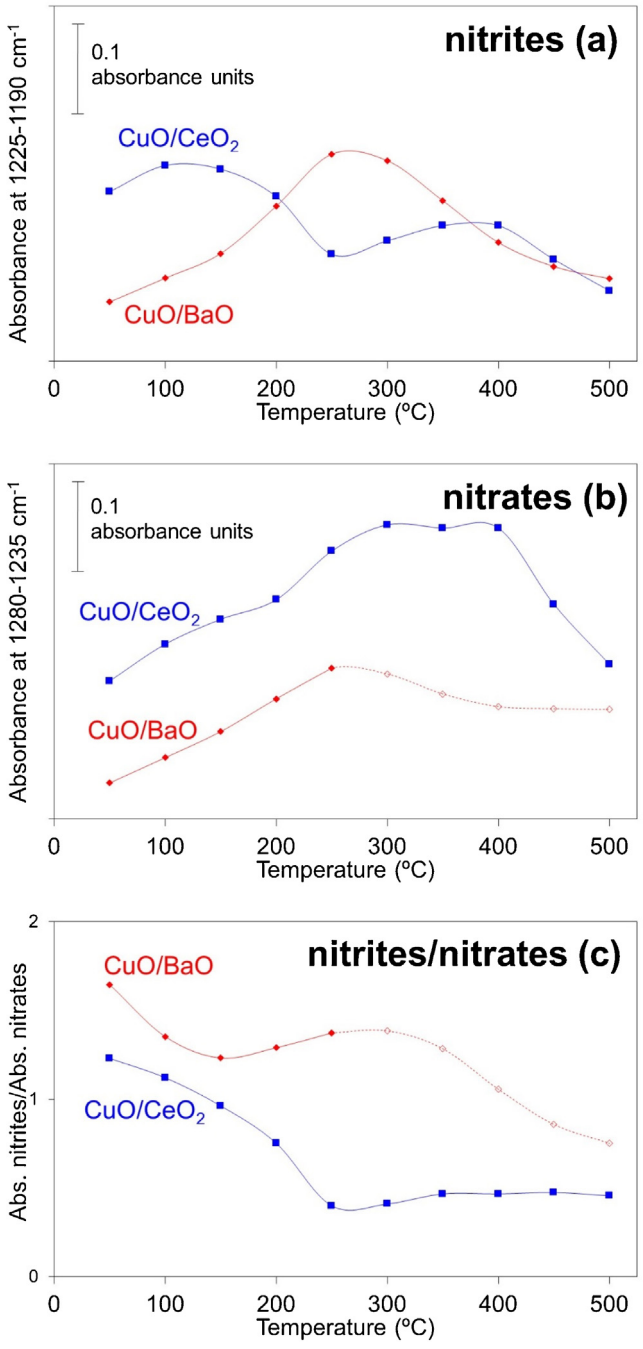

Fig. 4. Absorbance of nitrite (a) and nitrate (b) bands determined from spectra on Fig. 3 and nitrite to nitrate ratio (c).

their concentration decreased, consistent with the release of NOx observed above this temperature (Fig. 2a). The concentration of nitrates on CuO/CeO_2 (Fig. 4b) increased with temperature until 300 °C, with depletion only observed above 400 °C, in accordance with the release of NOx at high temperature (Fig. 2a). However, evidence of nitrate depletion was not observed in the 150–300 °C range. This suggests that there are two mechanisms by which NOx is chemisorbed on CuO/CeO_2. Adsorption of NOx at low temperature results in the formation of nitrites that decompose in the 150–300 °C range. The formation of nitrates is favored at higher temperature, which is in accordance with the increase in the catalyst oxidation capacity (Fig. 2b), and nitrates remained stable on the catalyst until 400 °C. This behavior is confirmed in data presented in Fig. 4c, where the ratio between the absorbance of the

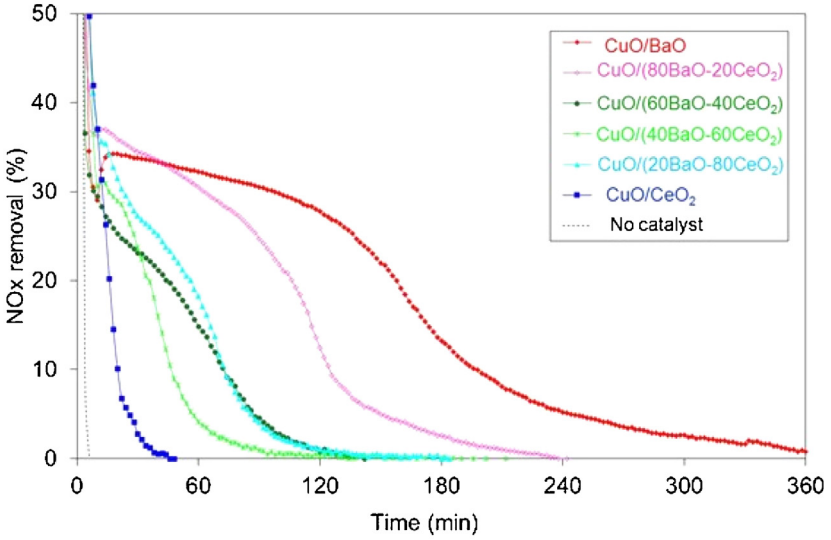

Fig. 5. NOx removal with time at 400 °C. (Gas mixture with 850 ppm NOx + 5%O_2 + N_2).

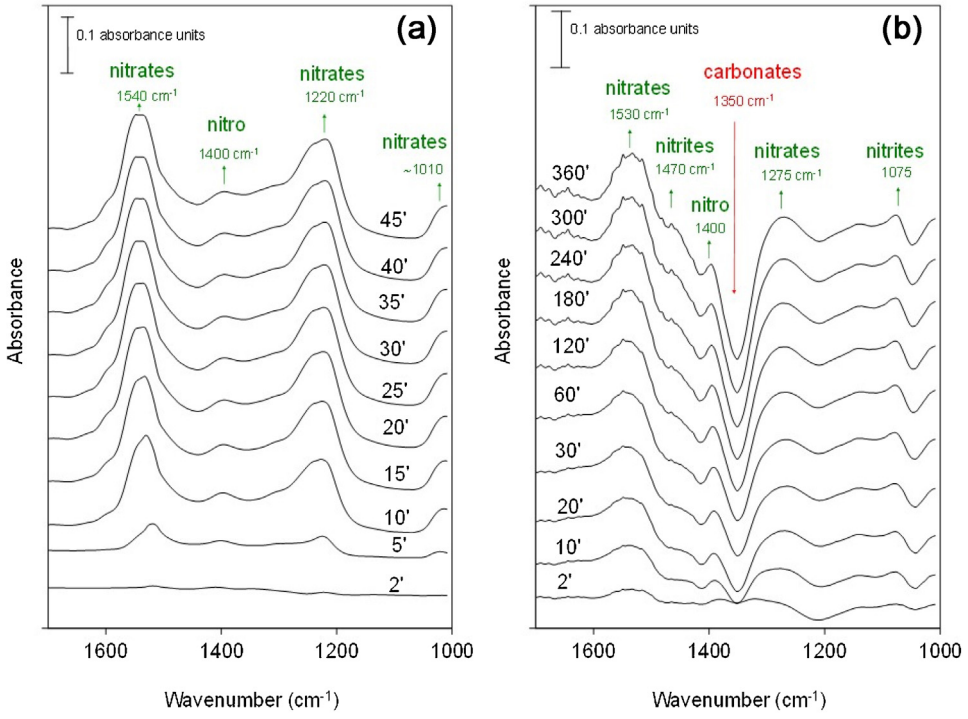

Fig. 6. Spectra obtained with CuO/CeO_2 (a) and CuO/BaO (b) and recorded during the Isothermal experiments at 400 °C. (Gas mixture with 850 ppm NOx + 5%O_2 + N_2).

nitrite and nitrate bands is shown as a function of temperature. The nitrite/nitrate ratio on the CuO/CeO_2 catalyst decreased from room temperature until 250 °C and remained stable above this temperature.

The evolution of the nitrogen oxide species chemisorbed on CuO/BaO followed a different pattern. The amount of nitrites and nitrates accumulated on CuO/BaO below 200 °C was much lower than that observed on CuO/CeO_2, and this was in agreement with the NOx profiles (Fig. 2a). The CuO/BaO catalyst chemisorbed detectable amounts of NOx above 250 °C (Fig. 2a), and above this temperature, surface nitrites disappeared (Fig. 4a). This suggested that the increased chemisorption above this temperature was related to the formation of nitrates, although unfortunately, this could not be confirmed by DRIFTS (Fig. 4b) due to carbonates interference. The slight increase of the NO_2 concentration observed above 200 °C (Fig. 2b) suggested that the CuO/BaO catalyst was able to oxidize NO above this temperature, and surface nitrites were simultaneously oxidized to surface nitrates. Once this occurs, the NOx chemisorption capacity of CuO/BaO increases.

As a summary of the temperature programmed NOx storage experiments, it can be concluded that, for the purpose of the NSR technology, the maximum operating temperature for CuO/CeO_2 is 400 °C, because the stored NOx species decompose above this threshold. At 400 °C, CuO/CeO_2 showed high oxidation capacity (the NO_2 profile reached the thermodynamic equilibrium under the experimental conditions of this study) and NOx was stored on the catalyst mainly in the form of nitrates. On the contrary, CuO/BaO is not suitable for NSR below 250 °C, due to its low oxidation activity

Table 2
Amount of NOx stored on the catalysts at 400 °C.

	NOx stored at 400 °C(μmolNOx/$g_{catalyst}$)
CuO/CeO_2	168
$CuO/(20BaO\text{-}80CeO_2)$	437
$CuO/(40BaO\text{-}60CeO_2)$	281
$CuO/(60BaO\text{-}40CeO_2)$	343
$CuO/(80BaO\text{-}20CeO_2)$	779
CuO/BaO	1204

and its negligible NOx storage capacity. However, CuO/BaO did not exhibit temperature restrictions until 500 °C, which was the maximum temperature employed in this study. Finally, the behavior of catalysts with $(xBaO\text{-}(1\text{-}x)CeO_2)$ supports was between those described for CuO/CeO_2 and CuO/BaO. These conclusions lead us to select 400 °C for further assessment of the NSR process under isothermal conditions.

3.3. Isothermal NOx storage at 400 °C

Fig. 5 compiles the NOx removal profiles obtained with the different catalysts at 400 °C and Table 2 the amounts of NOx stored. These quantitative results were determined using the chemiluminiscence analyser.

The highest NOx storage capacity was obtained with CuO/BaO (1204 μmolNOx/$g_{catalyst}$), the lowest corresponded to CuO/CeO_2 (168 μmolNOx/$g_{catalyst}$), and the performance of catalysts with $(xBaO\text{-}(1\text{-}x)CeO_2)$ supports was between those of CuO/CeO_2 and CuO/BaO (281–779 μmolNOx/$g_{catalyst}$). The amounts reported in the literature for reference catalysts are, for example, 324 μmolNOx/$g_{catalyst}$ for $1\%Pt\text{–}20\%Ba/Al_2O_3$ [30] and 714 μmolNOx/$g_{catalyst}$ for a $1\%Pt\text{–}10\%Ba/Al_2O_3$ [31] also at 400 °C. These values indicate that CuO/CeO_2 presents lower NOx storage capacity than the reference materials, which is reasonable given that (i) the NO oxidation capacity of Pt is higher to that of CuO (and NO_2 is chemisorbed better than NO) and (ii) the NOx storage capacity of ceria is lower than that of $BaO/BaCO_3$. On the other hand, CuO/BaO attains higher NOx storage amounts than the reference materials because BaO was not diluted with alumina.

DRIFTS obtained with CuO/CeO_2 and CuO/BaO during the isothermal NOx storage experiments are compiled in Fig. 6a and b, respectively. After a few minutes under reaction conditions, CuO/CeO_2 showed three bands at 1540, 1220 and 1010 cm^{-1}, which were consistent with the presence monodentate and/or bidentate nitrates. A poorly defined band was also observed at 1400 cm^{-1} that could be ascribed to nitro groups. This behavior was consistent with the conclusions of the temperature programmed experiments, and confirmed that the good oxidation capacity of the CuO/CeO_2 catalyst leads to the storage of oxidized nitrogen oxide species. Note that the oxidation state of nitrogen in NO, which is the main nitrogen oxide on the gas fed, is +2 while the oxidation state in the stored species is +4 (nitro groups) and +5 (nitrates). The spectra obtained with $CuO/(20BaO\text{-}80CeO_2)$, $CuO/(40BaO\text{-}60CeO_2)$ and $CuO/(60BaO\text{-}40CeO_2)$, (not shown for the sake of brevity), were qualitatively similar to those of Cu/CeO_2, with monodentate and/or bidentate nitrate bands at 1550-1545, 1260-1250 and around 1000 cm^{-1}, and the nitro band at 1390–1370 cm^{-1}. However, the relative intensity of the bands depended significantly on the sample, as will be discussed later.

The spectra obtained with CuO/BaO (Fig. 6b) and $CuO/(80BaO\text{-}20CeO_2)$ (not shown) presented more bands than those of catalysts with higher loading of ceria. In addition to the nitrate bands at 1530 and 1275 cm^{-1}, and the nitro band at 1400 cm^{-1}, these two catalysts also showed bands at 1470 and 1075 cm^{-1} that could be attributed to monodentate nitrites. The presence of nitrites, with nitrogen in +3 oxidation state, was consistent with the lower oxidation capacity of the barium-rich catalysts with respect to those with high cerium content. This conclusion is consistent with DRIFTS studies carried out with commercial $Pt\text{-}Rh/BaO/Al_2O_3$ catalysts [32], where it was concluded that NO was initially chemisorbed as nitrites on BaO. Once NO_2 was formed by NO oxidation on the noble metals, this species was chemisorbed either molecularly forming nitrates or dissociatively forming nitrites and, after a certain concentration of NOx is accumulated on the catalyst, surface nitrites were oxidized to surface nitrates by NO_2. It has been also reported that nitrites are preferably formed on $Ba\text{-}Pt/Al_2O_3$ while nitrate formation is favored by addition of ceria to this catalyst due to the enhanced oxidation capacity [7].

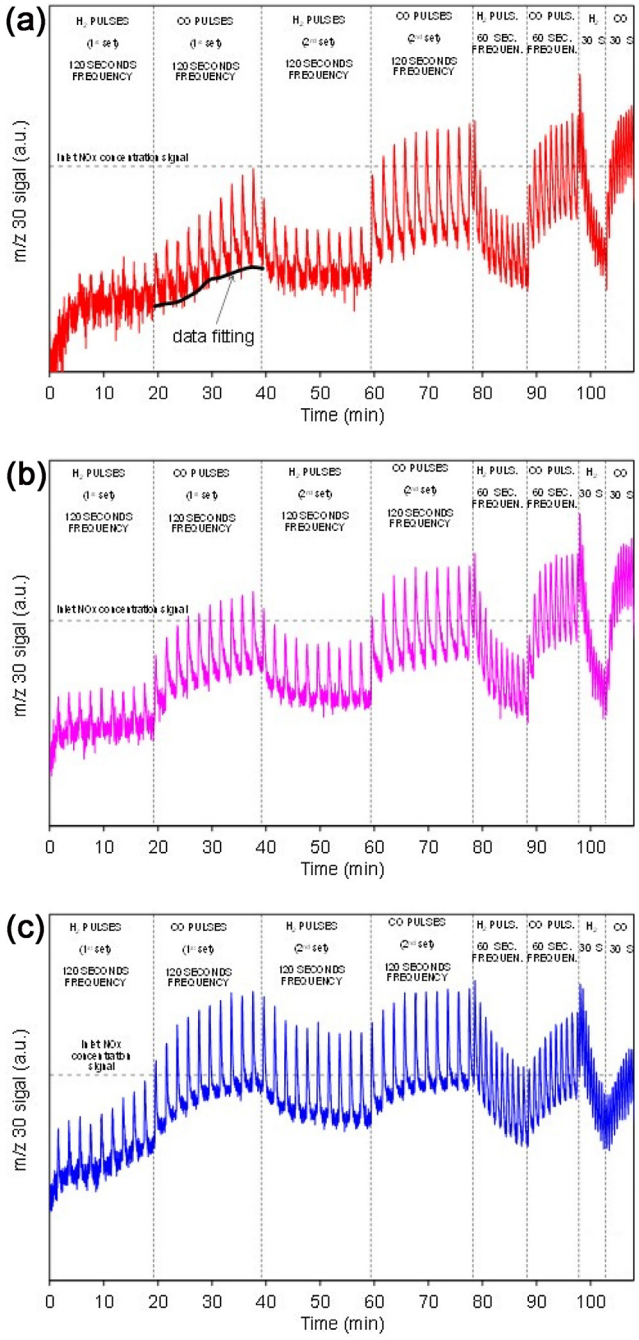

Fig. 7. NOx concentration monitored by *m*/*z* 30 mass spectrometry signal during NOx storage and reduction experiments performed at 400 °C. (a) CuO/BaO, (b) $CuO/(20BaO\text{-}80CeO_2)$ and (c) CuO/CeO_2.

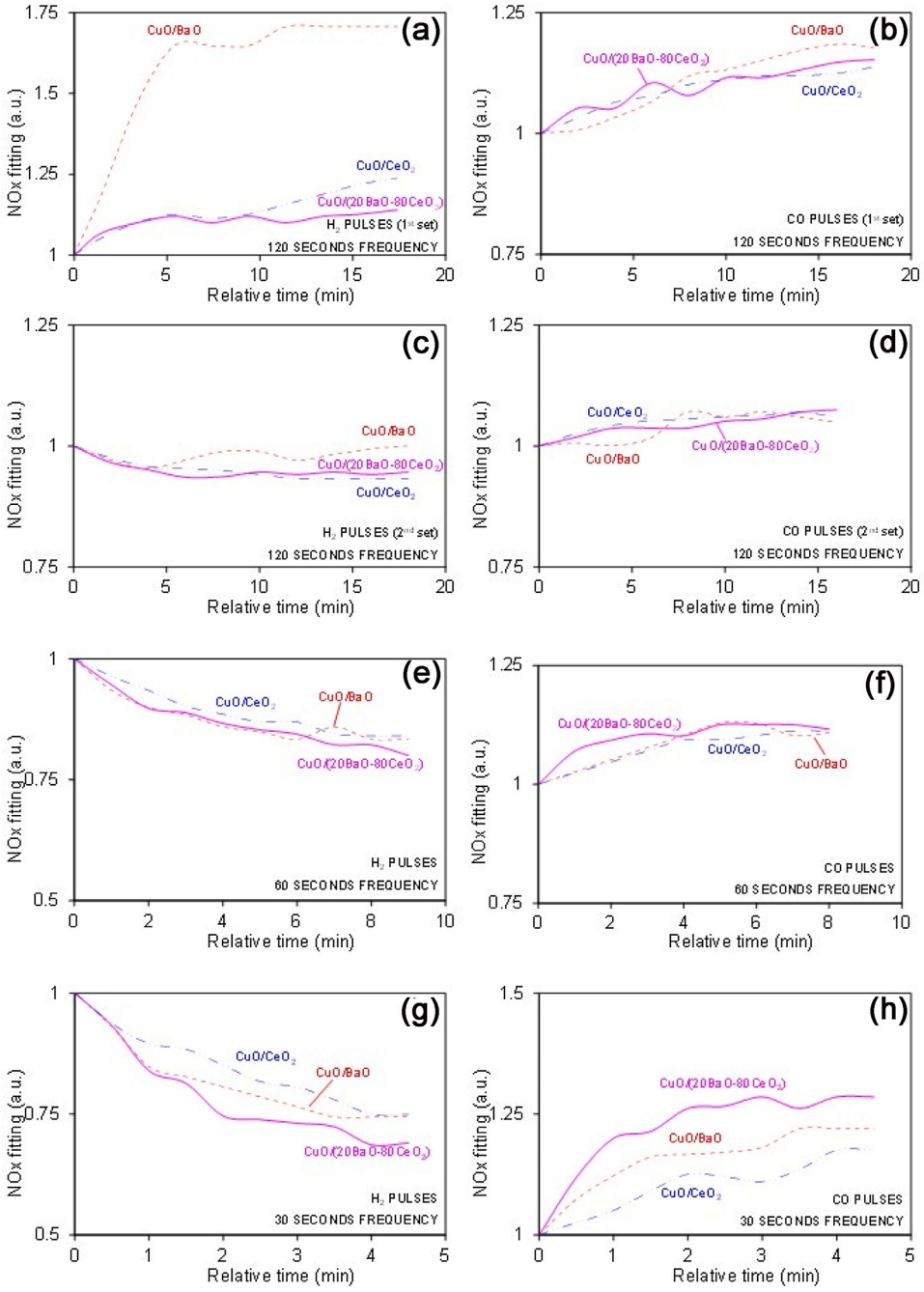

Fig. 8. NOx data of Fig. 7 fitting. NOx concentration at the beginning of each pulse was taken for the fitting, and concentrations were normalized by dividing all data of each series by the NOx concentration of the first point of the series. The time scales were set considering time = 0 at the beginning of the first pulse of each series. (a) H_2 pulses (1st set) 120 s frequency, (b) CO pulses (1st set) 120 s frequency, (c) H_2 pulses (2nd set) 120 s frequency, (d) CO pulses (2nd set) 120 s frequency, (e) H_2 pulses 60 s frequency, (f) CO pulses 60 s frequency, (g) H_2 pulses 30 s frequency and (h) CO pulses 30 s frequency.

Finally, the CuO/BaO catalyst (Fig. 6b), and to a lesser extent also CuO/(80BaO-20CeO_2) (not shown), showed evidence of carbonate decomposition with a band at 1350 cm^{-1} decreasing in intensity. This displacement of carbonates by nitrogen oxides occurred during isothermal conditions to a lesser extent than in those carried out under temperature programed conditions, because carbonates were partially removed while heating to 400 °C in inert gas.

3.4. Isothermal NOx storage and reduction (NSR) at 400 °C

NOx storage and reduction experiments were performed at 400 °C with selected catalysts under the same conditions as the isothermal experiments described in the previous section, but by additionally feeding pulses of CO or H_2 at different frequencies. Fig. 7 shows the *m*/*z* 30 signal followed by mass spectrometry which was used to monitor NOx concentration during the NSR experiments.

The profile shape of the *m*/*z* 30 signal consisted of peaks that followed the frequency of the reductant pulses and are attributed to NOx slip, that is, part of the NOx stored on the catalyst is reduced to N_2 but a fraction is released without undergoing reduction. In practical application, operation conditions must be optimized to maximise NOx reduction and minimise NOx slip.

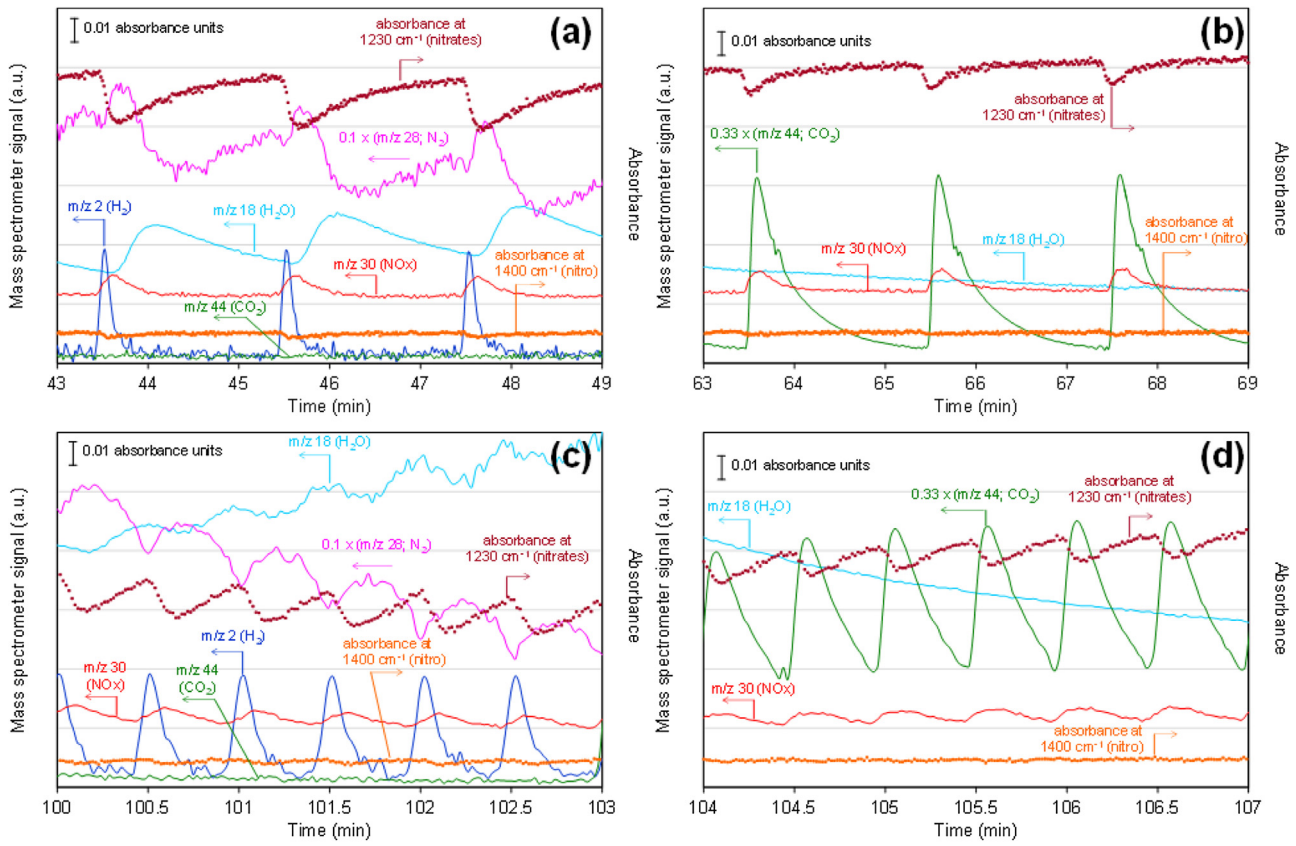

Fig. 9. Details of the NOx storage and reduction experiments performed at 400 °C with CuO/CeO_2. (a) H_2 pulses with 120 s frequency, (b) CO pulses with 120 s frequency, (c) H_2 pulses with 30 s frequency and (d) CO pulses with 30 s frequency. Time scale in X axis is equal to that on Fig. 7c. The baseline of the *m/z* 28 signal has been subtracted before plotting.

The NSR performance was mainly dependent on the nature of the reducing gas, on the pulsing frequency and, only under certain circumstances, on the nature of the copper catalyst. As a general observation, H_2 regeneration was more effective than using CO. In all cases the *m/z* 30 signal followed an increasing trend while exposing to CO pulses, which indicated that the catalysts were not fully regenerated by CO, and therefore, the NOx chemisorption capacity decreased with time. On the other hand, with the exception of the first set of H_2 pulses, the *m/z* 30 signal followed a decreasing trend with increasing number of H_2 pulses because, in this case, the catalysts were being more fully regenerated. The difference between the efficiency of CO and H_2 became more apparent for high frequency pulses, as expected. The better regeneration capacity of H_2 with regard to CO was also reported in previous studies for $Pt/Ba/Al_2O_3$ catalysts [6,33,34].

In order to analyze the trends shown in Fig. 7 in greater detail, curve fitting to the NOx data was manually performed as shown in the example in Fig. 7a (1st set of CO pulses with 120 s frequency). The NOx concentration at the beginning of each pulse was taken for the fitting, and trend lines were obtained. These trend lines are included in Fig. 8 after normalization by dividing all data corresponding to each trend line by the NOx concentration of the first point of each series, that is, all trend lines start with a value of 1, and relative changes are shown. Also, the time scales used in Fig. 8 were set by considering time = 0 min at the beginning of the first pulse of each series.

The main differences among the series of catalysts were observed during the first set of H_2 pulses (Fig. 8a), where CuO/BaO loses storage capacity much more rapidly than CuO/CeO_2 and $CuO/(20BaO\text{-}80CeO_2)$. However, the catalysts behavior at a later stage was quite similar, except in the case where CO was pulsed at a frequency of 30 s (Fig. 8h), where CuO/CeO_2 lost storage capacity slower than the other catalysts.

Catalysts regeneration was studied by rapid-scan DRIFTS. Fig. 9 presents the absorbance at selected wavenumbers together with *m/z* signals corresponding to gas species involved in the reactions for the CuO/CeO_2 catalyst. The selected wavenumbers allow nitrates (1230 cm^{-1}) and nitro groups (1400 cm^{-1}) to be continuously monitored, the latter having marginal participation in the reactions. Additional features corresponding to nitrites or carbonate/bicarbonate species where not observed during the NSR experiment performed with CuO/CeO_2.

The *m/z* signals monitored during the NSR experiment carried out with CuO/BaO are compiled in Fig. 10. In contrast to observations for CuO/CeO_2, the intensity of the main DRIFTS bands obtained with CuO/BaO did not follow the shape of the gas phase peaks, and for this reason are not included in Fig. 10. On the contrary, broad bands were obtained, and as an example, Fig. 11 shows the trend of one of the nitrate bands (at 1545 cm^{-1}) as a function of time for the complete NSR experiment. In the experiment performed using CuO/BaO, nitrite, nitro or carbonate/bicarbonate bands were also absent or negligible in intensity when compared with features due to nitrates.

The different shape of the *m/z* 30 curves indicates that the NOx chemisorption and desorption rates were much faster for CuO/CeO_2 (Fig. 10) than for CuO/BaO (Fig. 11). The faster chemisorption of CuO/CeO_2 is probably linked to its higher oxidation capacity (Fig. 2b) and the faster desorption rate explained on the basis of the lower stability of the chemisorbed species (see Fig. 2b).

For the CuO/CeO_2 catalyst (Fig. 9), the nitrate band at 1230 cm^{-1} followed a trend opposed to that of the gases pulsed, in that once H_2 or CO were introduced, the band due to nitrates decreased in

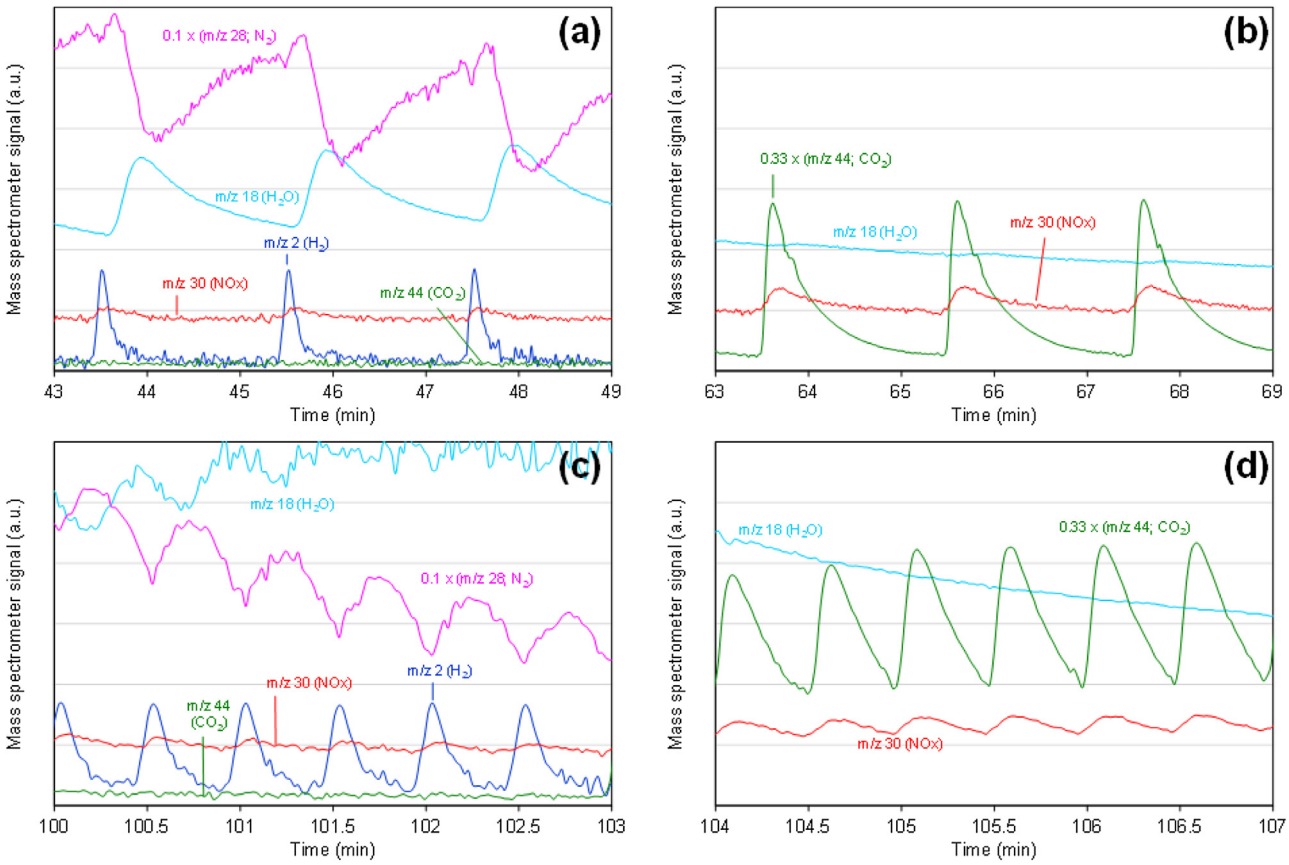

Fig. 10. Details of the NOx storage and reduction experiments performed at 400 °C with CuO/BaO. (a) H_2 pulses with 120 s frequency, (b) CO pulses with 120 s frequency, (c) H_2 pulses with 30 s frequency and (d) CO pulses with 30 s frequency. Time scale in X axis is equal to that on Fig. 7a. The baseline of the *m*/*z* 28 signal has been subtracted before plotting.

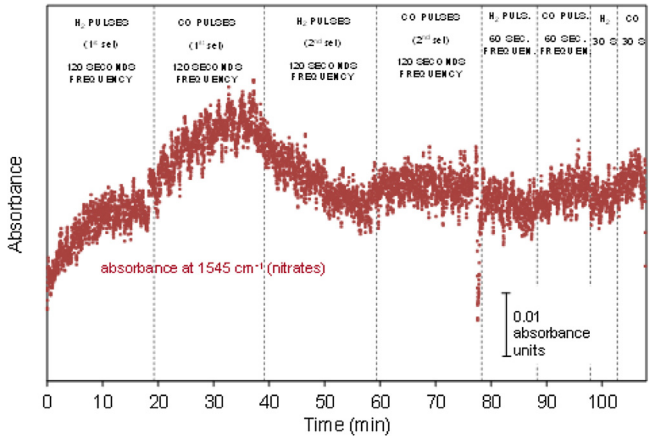

Fig. 11. Nitrates absorbance monitored by DRIFTS during NSR experiments performed at 400 °C with CuO/BaO.

intensity. The maxima of the *m*/*z* 28 signal match the nitrate band minima, confirming the release of N_2 upon catalyst surface regeneration. This was confirmed for H_2 pulses, but not for CO pulses because, in this case, both CO and N_2 contribute to the *m*/*z* 28 signal impeding the analysis of the reaction products. It is worth noting that evidence of other reduction by-products, such as N_2O (*m*/*z* 44) or NH_3 (*m*/*z* 17) were not observed under any experimental conditions. The general trend of the nitrate band intensity depended on the reductant pulsed, in agreement with previous conclusions. The concentration of nitrates on the CuO/CeO_2 catalyst showed a net decrease upon consecutive pulses of H_2, while the opposite trend was observed using CO pulses. These general trends were more apparent when employing a pulse frequency of 30 than 120 s, consistent with the fact that these processes are relatively slow and thus are less complete as the time period is reduced. These observations confirm that H_2 was much more effective compared with CO in cleaning chemisorbed NOx species from the catalysts.

For both catalysts studied (CuO/CeO_2 in Fig. 9 and CuO/BaO in Fig. 10), peaks indicating NOx slip appeared simultaneously with the H_2O or CO_2 peaks, which are reaction products of H_2 and CO oxidation, respectively. Not all of the H_2 pulsed reacted, and the unreacted fraction also yielded H_2 peaks which appeared simultaneously with those of the NOx and H_2O. Note that the H_2O peaks appeared delayed with respect to those of the H_2, NOx and nitrates peaks, while CO_2 peaks were not delayed with respect to NOx and nitrates. It was therefore concluded that H_2O interacted more strongly with the catalysts than CO_2. This may be explained on the basis that NOx and CO_2, both compete for the same chemisorption sites on the catalyst surface, and the fed of NOx in the gas phase hinders CO_2 chemisorption. This observation, together with the absence of carbonate/bicarbonate bands in the DRIFT spectra recorded during the NSR experiments upon CO pulses, rules out the possibility that the lower regeneration capacity of CO with regard to H_2 is related with the poisoning effect of the reaction products. On the contrary, it is suggested that H_2 regenerates the catalysts much better than CO due to its higher reactivity, as previously observed for $Pt/Ba/Al_2O_3$ [6].

In summary, the NSR experiments allow one to conclude that the general behavior of all catalysts tested (CuO/BaO, CuO/CeO_2 and $CuO/(20BaO\text{-}80CeO_2)$) was quite similar, and only certain differences were observed upon application of high frequency pulses of

CO, where CuO/CeO_2 showed better resistance to deactivation than the others. In general, H_2 regeneration was more effective than CO in terms of extent of regeneration, and this was attributed to the higher reactivity of H_2 rather than to any poisoning effect of the reaction products (H_2O and CO_2, respectively). Nitrates were the main chemisorbed nitrogen oxides under the NSR experimental conditions, and NOx chemisorption and desorption rates seemed to be faster for CuO/CeO_2 than for CuO/BaO.

4. Conclusions

The NSR behavior of copper catalysts was studied by operando DRIFTS-MS-Chemiluminiscence, and CeO_2, BaO and $BaO + CeO_2$ supports were compared. The following conclusions can be drawn:

- The maximum temperature for CuO/CeO_2 application in NSR is 400 °C, because stored NOx species decomposed above this temperature. At this temperature, CuO/CeO_2 showed high NO oxidation capacity and NOx was stored on the catalyst mainly forming nitrates and to a much lesser extent, nitro groups. On the other hand, CuO/BaO is not suitable for NSR below 250 °C, because its oxidation capacity was very low and its NOx storage capacity was negligible. However, CuO/BaO did not exhibit temperature restrictions until 500 °C. The effect of temperature on the behavior of copper catalysts with $BaO + CeO_2$ mixed oxide supports for NOx chemisorption was between those of CuO/CeO_2 and CuO/BaO.
- The general behavior of all catalysts tested for NSR at 400 °C (CuO/BaO, CuO/CeO_2 and $CuO/(20BaO\text{-}80CeO_2)$) was quite similar, and only specific differences were observed when using high frequency (every 30 s) pulses of CO, whereby CuO/CeO_2 showed the best resistance towards the decrease in NOx removal with time. For all catalysts, N_2 was the only NOx reduction product detected during H_2 regeneration.
- Catalysts regeneration with H_2 was more effective than CO regeneration for NSR experiments at 400 °C, and this was attributed to the higher reactivity of H_2 rather than to any poisoning effect of the reaction products (H_2O and CO_2, respectively). Nitrates were the main chemisorbed nitrogen oxide species formed on the catalyst and released under experimental conditions, and NOx chemisorption and desorption rates were faster for CuO/CeO_2 than for CuO/BaO.

Acknowledgements

The authors thank the financial support of Generalitat Valenciana (Project PROMETEOII/2014/010 and grant BEST/2014/250), the Spanish Ministry of Economy and Competitiveness (Projects CTQ2015-67597-C2-2-R, MAT2014-61992-EXP, and grant PRX14/00249), and the UE (FEDER funding). We thank Dr A.J. McCue (University of Aberdeen) for assistance involving the experimental set-up.

Appendix A. Supplementary data

Supplementary data associated with this article can be found, in the online version, at http://dx.doi.org/10.1016/j.apcatb.2016.05.067.

References

[1] W.S. Epling, L.E. Campbell, A. Yezerets, N.W. Currier, J.E. Parks II, Catal. Rev. Sci. Eng. 46 (2004) 163–245.
[2] Z. Liu, S. Ihl Woo, Catal. Rev. Sci. Eng. 44 (2006) 43–89.
[3] G. Liu, P.-X. Gao, Catal. Sci. Technol. 1 (2011) 552–568.
[4] S. Roy, A. Baiker, Chem. Rev. 109 (2009) 4054–4091.
[5] N. Takahashi, K. Yamazaki, K. Sobukawa, H. Shinjoh, Appl. Catal. B 70 (2007) 198–204.
[6] Z. Liu, J.A. Anderson, J. Catal. 224 (2004) 18–27.
[7] B. Pereda-Ayo, U. De La Torre, M.P. González-Marcos, J.R. González-Velasco, Catal. Catal. Today 241 (2015) 133–142.
[8] M. Casapu, J.-D. Grunwaldt, M. Maciejewski, F. Krumeich, A. Baiker, M. Wittrock, S. Eckhoff, Appl. Catal. B 78 (2008) 288–300.
[9] N. Maeda, A. Urakawa, A. Baiker, J. Phys. Chem. C 113 (2009) 16724–16735.
[10] R. Strobel, F. Krumeich, S.E. Pratsinis, A. Baiker, J. Catal. 243 (2006) 229–238.
[11] V. Rico-Pérez, A. Bueno-López, D.J. Kim, Y. Jib, M. Crocker, Appl. Catal. B 163 (2015) 313–322.
[12] R. Vijay, R.J. Hendershot, S.M. Rivera-Jimenez, W.B. Rogers, B.J. Feist, C.M. Snively, J. Lauterbach, Catal. Commun. 6 (2005) 167–171.
[13] A.E. Palomares, A. Uzcategui, A. Corma, Catal. Today 137 (2008) 261–266.
[14] E.C. Corbos, M. Haneda, X. Courtois, P. Marecot, D. Duprez, H. Hamada, Catal. Commun. 10 (2008) 137–141.
[15] F.E. López-Suárez, M.J. Illán-Gómez, A. Bueno-López, J.A. Anderson, Appl. Catal. B 104 (2011) 261–267.
[16] N. Takahashi, H. Shinjoh, T. Iijima, T. Suzuki, K. Yamazaki, K. Yokota, H. Suzuki, N. Miyoshi, S. Matsumoto, T. Tanizawa, T. Tanaka, S. Tateishi, K. Kasahara, Catal. Today 27 (1996) 63–69.
[17] J.P. Breen, C. Rioche, R. Burch, C. Hardacre, F.C. Meunier, Appl. Catal. B 72 (2007) 178–186.
[18] A. Davó-Quiñonero, A. Bueno-López, D. Lozano-Castelló, A.J. McCue, J.A. Anderson, Rapid-scan operando infrared spectroscopy, ChemCatChem (2016), http://dx.doi.org/10.1002/cctc.201600302.
[19] C. Mondelli, V. Dal Santo, A. Trovarelli, M. Boaro, A. Fusi, R. Psaro, S. Recchia, Catal. Today 113 (2006) 81–86.
[20] H. Li, M. Rivallan, F. Thibault-Starzyk, A. Travert, F.C. Meunier, Phys. Chem. Chem. Phys. 15 (2013) 7321–7327.
[21] J.P. Breen, R. Burch, C. Fontaine-Gautrelet, C. Hardacre, C. Rioche, Appl. Catal. B 81 (2008) 150–159.
[22] N. Guillén-Hurtado, A. Bueno-López, A. García-García, J. Mater. Sci. 47 (2012) 3204–3213.
[23] K. Krishna, A. Bueno-López, M. Makkee, J.A. Moulijn, Appl. Catal. B 75 (2007) 210–220.
[24] M. AL-Harbi, W.S. Epling, Catal. Lett. 130 (2009) 121–129.
[25] W.S. Epling, C.H.F. Peden, J. Szanyi, J. Phys. Chem. C 112 (2008) 10952–10959.
[26] J. Dupré, P. Bazin, O. Marie, M. Daturi, X. Jeandel, F. Meunier, Appl. Catal. B 181 (2016) 534–541.
[27] J. Dupré, P. Bazin, O. Marie, M. Daturi, X. Jeandel, F. Meunier, Appl. Catal. B 160–161 (2014) 335–343.
[28] K.I. Hadjiivanov, Catal. Rev. Sci. Eng. 42 (2000) 71–144.
[29] D. Gamarra, A. Martínez-Arias, J. Catal. 263 (2009) 189–195.
[30] L. Lietti, P. Forzatti, I. Nova, E. Tronconi, J. Catal. 204 (2001) 175–191.
[31] Z. Liu, J.A. Anderson, J. Catal. 224 (2004) 18–27.
[32] Ch. Sedlmair, K. Seshan, A. Jentys, J.A. Lercher, J. Catal. 214 (2003) 308–316.
[33] D. James, E. Fourré, M. Ishii, M. Bowker, Appl. Catal. B 45 (2003) 147–159.
[34] T. Szailer, J.H. Kwak, D.H. Kim, J.C. Hanson, Charles H.F. Peden, J. Szanyi, J. Catal. 239 (2006) 51–64.